



Published in final edited form as:

Transl Res. 2015 December ; 166(6): 554–567. doi:10.1016/j.trsl.2015.09.004.

Therapeutic Benefits of Young, But Not Old, Adipose-Derived Mesenchymal Stem Cells in a Chronic Mouse Model of Bleomycin-Induced Pulmonary Fibrosis

Jun Tashiro, MD, MPH^{1,*}, Sharon J. Elliot, PhD^{1,*}, David J. Gerth, MD¹, Xiaomei Xia, BS², Simone Pereira-Simon, BS¹, Rhea Choi, BS², Paola Catanuto, PhD¹, Shahriar Shahzeidi, MD³, Rebecca L. Toonkel, MD⁴, Rahil H. Shah², Fadi El Salem, MD⁵, and Marilyn K. Glassberg, MD^{1,2,3}

¹Department of Surgery, Leonard M. Miller School of Medicine, University of Miami, Miami, FL, USA

²Division of Pulmonary, Critical Care, Allergy, and Sleep Medicine, Department of Medicine, Leonard M. Miller School of Medicine, University of Miami, Miami, FL, USA

³Division of Pediatric Pulmonology, Department of Pediatrics, Leonard M. Miller School of Medicine, University of Miami, Miami, FL, USA

⁴Department of Medicine, Herbert Wertheim College of Medicine, Florida International University, Miami FL, USA

⁵Department of Pathology, Icahn School of Medicine at Mount Sinai, New York, NY, USA

Abstract

The observation that pulmonary inflammatory lesions and bleomycin (BLM)-induced pulmonary fibrosis spontaneously resolve in young mice, while remaining irreversible in aged mice, suggests that impairment of pulmonary regeneration and repair is associated with aging. Since mesenchymal stem cells (MSCs) may promote repair following injury, we postulated that differences in MSCs from aged mice may underlie post-injury fibrosis in aging. The potential for young-donor MSCs to inhibit BLM-induced pulmonary fibrosis in aged male mice (>22 months) has not been studied. Adipose-derived MSCs (ASCs) from young (4-month) and old (22-month) male mice were infused 1-day following intratracheal BLM administration. At 21-day sacrifice, aged BLM mice demonstrated lung fibrosis by Ashcroft score, collagen content, and α_v -integrin mRNA expression. Lung tissue from aged BLM mice receiving young ASCs exhibited decreased fibrosis, matrix metalloproteinase (MMP)-2 activity, oxidative stress, and markers of apoptosis vs. BLM controls. Lung mRNA expression of TNF α was also decreased in aged BLM mice receiving

Corresponding author/address for reprints: Marilyn K. Glassberg MD, Professor of Medicine and Surgery, University of Miami Miller School of Medicine, 1550 NW 10th Avenue, Suite 411, Miami, FL 33136. Phone: +1 (305) 243-3709, Fax: +1 (305) 243-3738. mglassbe@med.miami.edu.

*Jun Tashiro and Sharon J. Elliot contributed to this project equally.

Disclaimers: None, for all authors.

Publisher's Disclaimer: This is a PDF file of an unedited manuscript that has been accepted for publication. As a service to our customers we are providing this early version of the manuscript. The manuscript will undergo copyediting, typesetting, and review of the resulting proof before it is published in its final form. Please note that during the production process errors may be discovered which could affect the content, and all legal disclaimers that apply to the journal pertain.

young-donor ASCs vs. BLM controls. In contrast, old-donor ASC treatment in aged BLM mice did not reduce fibrosis and related markers. On examination of the cells, young-donor ASCs had decreased mRNA expression of MMP-2, insulin-like growth factor receptor, and AKT activation compared to old-donor ASCs. These results show that the BLM-induced pulmonary fibrosis in aged mice could be blocked by young-donor ASCs and that the mechanisms involve changes in collagen turnover and markers of inflammation.

Keywords

bleomycin; pulmonary fibrosis; idiopathic pulmonary fibrosis; stem cells; aging

Introduction

Idiopathic pulmonary fibrosis (IPF) is a progressive and debilitating lung disease characterized by interstitial fibrosis with decreasing lung volumes and pulmonary insufficiency eventually resulting in death. [1, 2] Approximately two-thirds of persons with IPF are aged 60 years or older at the time of diagnosis. The incidence and prevalence of IPF is significantly higher among men aged 55 years or older, compared with women of the same age. [3] Although recent approvals of pirfenidone and nintedanib hold promise for patients with early stage IPF, no curative treatments are available for this terminal and devastating disease. [4]

Most preclinical studies of IPF utilize the murine bleomycin (BLM) lung fibrosis model. This model is well characterized [5–16] and was recently shown to replicate the molecular changes seen in patients with active disease. [17]

While the murine BLM model is useful for preclinical studies, one of its limitations is the observed effect of age – when compared with young mice, aged mice develop more severe pulmonary fibrosis and have higher mortality rates in response to BLM exposure. [12, 13] Recent studies suggest that this may be explained by the fact that the lungs of young mice undergo spontaneous resolution of BLM fibrosis – whereas the fibrosis does not resolve in the lungs of aged mice. [16, 18] While the mechanism is unknown, it has been suggested that age-related variations in the activity of anti-inflammatory factors and matrix metalloproteinases (MMPs) may contribute. The source of these protective factors in the lungs of young mice is unclear, but may be related to the increased prevalence of endogenous stem cells or Type 2 pneumocytes (progenitor cells that regenerate the alveolar epithelium). [9, 19–24]

While studies to elucidate the potential of stem cell therapy in the BLM model have been performed on young mice using mesenchymal stem cells (MSCs) from bone-marrow or amniotic fluid, [6, 7, 25] no studies to date have examined the effects of donor stem cells from aged mice. This information is critical, since IPF is most common in older age. Using a model of lipopolysaccharide-induced lung injury, Bustos et al. showed that bone-marrow derived mesenchymal stem cells (BM-MSCs) from aged mice lack the anti-inflammatory protective effect of BM-MSCs from young mice. [19] Recent studies in the treatment of cognitive impairment of aged mice suggest that stem cell transplantation from young mice

may hold promise as a therapy to combat age-related change. [26, 27] In addition, Feng et al. have demonstrated that age-related renal damage was reversed by stem cell transplantation from young donors. [28] Based on these prior results, we investigated the effect of ASC donor age on BLM-induced pulmonary fibrosis by isolating adipose-derived mesenchymal stem cells (ASCs) from young (yASCs; 4 month) and aged (oASCs; 22 month) male mice in order to determine whether yASCs were more effective than oASCs against the development of BLM pulmonary fibrosis and elucidate possible therapeutic mechanisms.

Materials and methods

Animal model

Male C57BL/6 mice were obtained from the National Institute of Aging (Bethesda, MD). BLM lung fibrosis recipients were all 22 month old male C57BL/6 mice, with a small subanalysis performed on 4 month old male C57BL/6 mice. Animals were housed under specific pathogen-free conditions with food and water *ad libitum*. All experiments and procedures were approved by the Institutional Animal Care and Use Committee at the Leonard M. Miller School of Medicine at the University of Miami (Miami, FL), a facility accredited by the American Association for the Accreditation of Laboratory Animal Care.

BLM administration

After the administration of anesthesia, bleomycin sulfate (Sigma-Aldrich Corp; St. Louis, MO) dissolved in 50 μ l sterile saline at 2.5 U per kg of bodyweight was administered by direct intratracheal instillation via intubation. Control mice received 50 μ l of sterile saline using the same method. Mice were sacrificed at 21 days following BLM administration (Fig. 1).

ASC Isolation

Donor ASCs were isolated from the subcutaneous adipose pads of 4- and 22-month old C57BL/6 mice. Mice were anesthetized by a ketamine (200 mg/kg) and xylazine (10 mg/kg) injected intraperitoneally. Subcutaneous adipose tissue was excised, washed in phosphate buffer solution without Ca^{2+} and Mg^{2+} (PBS) containing 30% GIBCO® Pen/Strep (Life Technologies; Grand Island, NY) and digested in media containing 0.75% type II collagenase (Sigma-Aldrich; St. Louis, MO). The suspension was centrifuged to separate floating adipocytes from the stromal vascular fraction. The resultant pellet was resuspended and cultured in ADSC™ Growth Medium (Lonza Group Ltd; Basel, Switzerland). Cells were expanded in plastic Thermo Scientific™ Nunc™ Cell Culture Treated Flasks with Filter Caps (Thermo Fisher Scientific, Inc., Waltham, MA). After a 24-hr incubation period, non-adherent cells were removed. When the adherent cells became confluent, they were trypsinized, expanded for 2–3 passages and cryopreserved in Recovery™ Cell Culture Freezing Medium (Life Technologies).

Characterization of Stem Cells

ASCs were incubated with one of the fluorescence-labeled antibodies: Pacific Blue anti-CD90.2, Pacific Blue anti-CD205, FITC anti-CD29, PE anti-Sca1, FITC anti-CD79 α , APC-

Cy7 anti-CD45, PE anti-CD14, or PE anti-CD11. Cells were analyzed by flow-assisted cell sorting (FACS) Canto™ II (BD Biosciences; San Jose, CA). For differentiation, the Mouse Mesenchymal Stem Cell Functional Identification Kit (R&D Systems Inc.; Minneapolis, MN) was used according to the manufacturer's instructions. Pluripotency was assessed via osteogenic and adipogenic differentiation. [10]

Stem Cell injections

ASCs (passage 2 or 3) were thawed immediately prior to injection in a 37° C water bath and washed in PBS to remove the cell freezing solution. ASCs were passed through a 70 µm cell strainer to eliminate cell clumps. Cells were counted and resuspended in PBS in preparation for injection according to a modified version of a previously published protocol. [29] Twenty-four hours following BLM administration, each animal received 200 µl either PBS (control) or 5×10^5 ASCs (treated) in 200µl of PBS by tail vein injection over a 1 minute period. [30- 31] Control mice given intratracheal saline also received injections of donor ASC, as described above.

Lung tissue analysis/immunohistochemistry

Left lung lobes were harvested for protein, MMP, and mRNA analysis. For morphometry and histology studies, right lung lobes were inflated with 10% neutral buffered formalin (NBF) under 25 cm H₂O pressure. The lungs were postfixed by immersion in 10% NBF for 24 hours and then transferred to PBS at 4°C. Samples were paraffin-embedded and 4 µm sections were obtained for hematoxylin-eosin and Masson's Trichrome staining,

Ashcroft scoring

Pulmonary fibrosis was assessed by a pathologist blinded to the experimental groups using the semiquantitative Ashcroft method [32] on Masson's Trichrome-stained slides at 20× magnification. Individual fields were assessed by systematically moving over a 32-square grid; each field was assessed for fibrosis severity and assigned a score on a scale of 0 (normal lung) to 8 (total fibrosis of the field) and an average was obtained for each slide.

Collagen Content Assessment by Hydroxyproline Content

Hydroxyproline content was determined according to the manufacturer's instructions (Hydroxyproline Assay Kit; Sigma-Aldrich, St. Louis, MO). Briefly, 2 mg lung fragments were weighed and homogenized in 100 µl of distilled water. An equal volume of 10 N HCl was added to the samples before drying at 49° C for 3 hours. 50 µl of sample was loaded in the plate and incubated overnight at 37° C. A hydroxyproline standard curve was prepared according to a standard solution (between 0 and 1µg/well). Hydroxyproline content was read at 557 nm, using the SoftMax Pro Software (Molecular Devices Corp; Sunnyvale, CA).

Real-Time PCR

Amplification and measurement of target RNA was performed on the Step 1 real time PCR system as previously described. [33] Transforming growth factor β (TGF β), α_v -integrin, tumor necrosis factor alpha (TNF α), vascular endothelial growth factor (VEGF) and Nrf2 expression was measured using RNA extracted from lung tissues. In addition, MMP-2 and

insulin-like growth factor (IGF) receptor mRNA expression was assessed in yASCs and oASCs. The TaqMan rRNA control reagents kit (Life Technologies) was used to detect *18S* rRNA gene, an endogenous control, and samples were normalized to the *18S* transcript content as previously described. [34]

Bio-Plex

TGF β protein was quantitatively determined with the Bioplex platform as per manufacturer's recommendations (Bio-Rad). The same lysates collected for Bioplex were analyzed by western blotting, as described below, to validate the Bioplex platform.

Western Blot

Lung tissue was homogenized and western analysis was performed as previously described. [35] For Caspase-9, pAKT, AKT, and β -actin, 5 to 25 μ g of protein lysate was fractionated on 10% polyacrylamide gels. For TGF β analysis, 60 μ g of protein lysate was fractionated on a 12.5% gel. Immunoreactive bands were determined by exposing nitrocellulose blots to a chemiluminescence solution (Denville Scientific Inc.; Metuchen, NJ) followed by exposure to Amersham Hyperfilm ECL (GE Healthcare Limited; Buckinghamshire, UK). To determine the relative amounts of protein densitometry was evaluated using the Image J version 1.48v (National Institutes of Health; Bethesda, MD). All values from western blots were initially standardized to the corresponding β -actin band prior to comparative analyses.

MMP Activity

MMP-2 activity was assessed in lung tissue supernatants using a previously described method. [35] Briefly, Novex® 10% zymogram gels (Life Technologies) were incubated for 24 hours in a gelatinase solution, which allows the determination of total proteolytic MMP activities without interference from associated tissue inhibitors. Relative MMP activity was determined by densitometry using Image J (NIH).

Apoptosis Detection

Apoptosis was evaluated using the terminal deoxynucleotidyl transferase-mediated dUTP nick-end labeling (TUNEL) assay using the ApopTag fluorescein *in situ* apoptosis detection kit (Chemicon International; Temecula, CA). Counts were obtained by systematically moving a 25-field grid. Slides were moved and counted per section. Lung tissue was scored as apoptotic only when nuclear labeling by 4',6-diamidino-2-phenylindole (blue) and nuclear TUNEL labeling (green) co-localized, resulting in turquoise nuclei.

Reactive oxygen species (ROS)

One mg pieces of fresh lung tissue were cut placed in a 96-well plate. ROS was measured using 5- (and 6-) carboxy-2',7'-dichlorodihydrofluorescein diacetate (carboxy-H₂DCFDA) according to the manufacturer's instructions (Molecular Probes; Eugene, OR). ROS measurements were normalized by tissue sample weight for analysis.

Statistical Analysis

All values are expressed as mean \pm SEM. Overall significance of differences within experimental groups was determined by ANOVA in combination with Tukey's multiple-comparison test. Significance of differences between groups was determined using Student's *t*-tests, using Welch's correction as appropriate. *P* values less than 0.05 were considered significant.

Results

Assessment of underlying fibrosis in saline control mice

Mice (22 month) receiving saline instillations were compared to age-matched naïve mice for assessment as aged experimental controls. We found no differences in Ashcroft scoring, collagen content, or TNF α mRNA expression between naïve and saline control mice.

Characteristics of donor mice, donor ASCs and recipient mice

ASCs were isolated from both young (4 month) and aged (22 month) C57BL/6 male mice. Adherent cell had a homogenous fibroblastic morphology after 7 to 10 days in culture. By FACS analysis, the isolated ASCs demonstrated the well characterized expression pattern of mesenchymal markers including CD90.2⁺, CD105⁺, CD29⁺, Sca-1⁺, CD79 α ⁻, CD45⁻, CD14⁻, and CD11⁻ (Table 1). Both ASC lines demonstrated a high potential for osteogenic and adipogenic differentiation. Osteogenic and adipogenic differentiation were demonstrated at passage 2 (Fig. 2).

Recipient mice were 22 month old C57BL/6 males. Body weight did not differ between the groups of mice [Saline (n=8) 34.2 \pm 2.23 g, BLM (n=11) 29.7 \pm 1.83 g, BLM+yASC (n=7) 30.4 \pm 1.21 g, and BLM+oASC (n=10) 27.3 \pm 1.63 g]. In the present study, 2.5 U/kg of BLM was used, which resulted in a 4% mortality rate. Previous studies using one-time instillations of BLM between 1.25 [16] and 4 U/kg [6, 7] demonstrated high mortality rates when doses exceeded 3 U/kg. [17]

yASCs inhibit fibrosis in aged male mice receiving BLM

There was no evidence of pulmonary fibrosis (Ashcroft score) in histologic sections of control mice receiving saline, whereas the lungs of mice receiving BLM demonstrated alveolar wall thickening, increased interstitial and peri-vascular collagen deposition, and alveolar wall destruction with airspace enlargement (Fig. 3). Sham injections performed without cells or saline solution did not affect the development of BLM-induced pulmonary fibrosis. The severity of fibrosis by Ashcroft score was increased in animals receiving BLM (4.0 \pm 0.2) compared to saline controls (1.4 \pm 0.1, *****p*<0.0001; Fig. 4A). Importantly, the fibrosis score in lungs of mice receiving BLM (4.0 \pm 0.2) was decreased in those treated with yASCs (1.3 \pm 0.4, ***p*<0.005). However, the score in those treated with oASCs remained elevated (3.9 \pm 0.4). There was no difference in the fibrosis scores between saline controls and saline+yASC treatment (1.4 \pm 0.1 vs. 1.4 \pm 0.2).

The collagen content as assessed by hydroxyproline levels paralleled the histological findings. Namely, BLM treatment resulted in increased collagen levels (via hydroxyproline

assay) in old mice receiving BLM. This increase was blocked by injections of yASCs (* $p < 0.05$), but not by oASCs (Fig. 4B). In addition, α_v -integrin mRNA expression, another marker of pulmonary fibrosis, was also decreased in mice receiving BLM+yASCs compared to mice receiving BLM alone (*** $p < 0.001$) and those receiving BLM+oASCs (* $p < 0.05$), (Fig. 4C).

yASCs inhibit mRNA expression of molecular markers (TGF β , TNF α , VEGF-A) associated with BLM-induced fibrosis

Mice receiving BLM demonstrated increased expression of TGF β and TNF α mRNA, whereas this increase was blocked in mice that received BLM+yASC (Table 2). These findings were confirmed by BioPlex analysis; there was a BLM-induced increase in TGF β expression (5.84 \pm 0.78 pg/ml) vs. saline (2.04 \pm 1.01 pg/ml), $p < 0.05$. This increase was inhibited by yASC treatment (1.52 \pm 1.04 pg/ml), $p < 0.05$. Treatment with oASCs however, did not have the same effect. VEGF-A mRNA expression was decreased in the lungs of mice that received BLM. While treatment with yASCs increased VEGF-A mRNA expression, their levels did not reach (only ~22%) that of saline controls.

yASCs inhibit activation of MMP-2 and AKT

BLM instillation resulted in increased lung MMP-2 activity compared to lungs of saline control mice (Fig. 5A, * $p < 0.05$). Similar MMP-2 activity was noted in the lungs of mice receiving BLM+oASCs, but was not observed in the lungs of animals receiving BLM+yASCs (** $p < 0.01$) compared to BLM.

Increased phosphorylated AKT correlated with changes in MMP-2 activity between treatment groups (Fig. 5B). Lungs from mice receiving BLM had increased AKT activation (*** $p < 0.001$) compared to the lungs from mice receiving saline. Activation of AKT was lower in lungs of BLM+yASC mice (* $p < 0.05$) compared to lungs of mice receiving BLM, and did not differ from that of the lungs of saline controls.

yASCs maintain redox balance (ROS, Nrf2) and reduced levels of apoptosis (TUNEL, Caspase-9)

ROS levels did not differ between lungs from mice receiving saline or BLM. Lung tissue from mice receiving BLM treated with yASCs showed decreased ROS levels compared to lung tissue from all other groups (Table 2). BLM administration also led to decreased lung expression of Nrf2 in comparison to saline treatment. This BLM-induced decrease in expression in the mouse lungs was inhibited by treatment with yASCs, but not oASCs.

There was increased apoptotic activity in the lungs of mice receiving BLM compared to saline controls as demonstrated by TUNEL staining lung specimens on day 21 sacrifice (Fig. 6A). This BLM-induced increase was inhibited by treatment with yASCs, but not oASCs. Data obtained from TUNEL assays correlated with protein expression of cleaved caspase-9, also performed using lung specimens on day 21 sacrifice (Fig. 6B). BLM administration increased the ratio of cleaved caspase-9 to total caspase-9 compared to saline instillation (*** $p < 0.0001$), an effect which was inhibited by yASC treatment (*** $p < 0.001$). In addition, lung tissues from mice receiving BLM treated with oASCs showed increased

expression of cleaved caspase-9 relative to total caspase-9 compared to lung tissue from mice receiving BLM treated with yASCs (* $p < 0.05$) at similar levels to BLM.

MMP-2 activity and mRNA/protein expression of donor cells

There was a 100-fold increase in the expression of MMP-2 and MMP-9 mRNA in donor cells of the oASC line compared to the yASC line. Similarly, we found a 2-fold increase in the expression of α_v -integrin, and IGFR mRNA in the old ASC line compared to the yASC line. In addition, TGF β mRNA expression was elevated 1.5 fold in the old ASC line, compared to the yASC line.

Zymography revealed a 2 fold increase in MMP-2 activity in oASCs compared to yASCs. AKT activation was 3-fold higher in the old ASC cell lines compared to that of the yASC lines.

oASCs alters the course of bleomycin induced fibrosis in young mice

Young mice (4 month) receiving BLM were found to demonstrate the initial stages of resolving pulmonary fibrosis at day 21 sacrifice on evaluation of collagen content (4.59 ± 0.26). Treatment with oASC however, altered this phenomenon (5.69 ± 0.31), $p = 0.026$ (Fig. 7A). The findings were corroborated by the evaluation of integrin levels, where young mice receiving BLM (1.65 ± 0.12) had lower levels of each endpoint compared to young BLM mice injected with oASCs (3.22 ± 0.33), $p = 0.004$ (Fig. 7B). In addition, TGF β mRNA (young BLM mice [28.1 ± 4.20] vs. young BLM mice + oASCs [19.3 ± 2.75]) and protein (young BLM mice [5.96 ± 0.64 pg/mL] vs. young BLM mice + oASCs [9.25 ± 4.25 pg/mL]) did not differ between the groups.

Discussion

This is the first demonstration that a) adipose derived-MSCs inhibit BLM-induced pulmonary fibrosis in aged male C57BL/6 mice, b) the progressive pulmonary fibrosis in aged mice can be inhibited by ASCs from young, but not old, donors, and c) oASC administration to young mice prevents the resolution of BLM-induced pulmonary fibrosis.

We found that fibrosis (Ashcroft score, hydroxyproline, α_v -integrin) was significantly increased in the lungs of aged mice receiving BLM. These results agree with others who showed that collagen levels acutely increase in BLM-induced lung fibrosis in both young and aged mice. [5, 6, 10⁻¹³, 17] In addition, we confirm that increased collagen levels directly correlate with quantitative histologic examinations showing increased fibrotic deposition and architectural disruption in the lungs of mice receiving BLM, as well as the increased expression of the α_v -integrin subunit (associated with solid organ fibrosis) in BLM-induced pulmonary fibrosis. [5, 7, 8, 11⁻¹³, 17, 36]

Since IPF tends to affect older men, the fact that aged mice may have increased sensitivity to fibrosis from BLM instillation, due to age-related changes in the extracellular matrix (ECM) composition [37, 38] or an impaired ability of endogenous stem cells to confer protection against fibrosis, may demonstrate that aged mice more closely model IPF in humans. [5⁻⁷, 10, 17, 19] Comparisons of the response of aged and young mice to BLM reveal that aged

mice have significantly higher rates of BLM-induced mortality, collagen deposition, and destruction of alveolar epithelium on histologic examination. [12, 13, 16] Older mice also have increased levels of molecular markers of fibrosis, including Thy-1, [13, 37] IL-17A, CXCL1, and TGF- β . [12]

Until quite recently, many prior studies of BLM-induced pulmonary fibrosis were terminated 14 days after BLM instillation, where spontaneous resolution of BLM-induced fibrosis was not discussed. [6, 7, 11–13, 15–18] Since fibrosis after BLM plateaus in young mice at 21 days and begins the process of resolution thereafter, we chose this time point as the endpoint to study aged mice in the current study. [5, 16, 18, 39] As noted in our histologic evaluation and quantification of related markers, aged mice do not undergo the same phenomenon of spontaneous resolution of pulmonary fibrosis.

The finding that infusion of donor ASCs from young but not aged donor male mice inhibited the fibrotic response to BLM is the first in a study focusing on aged male mice after BLM. Although several studies have sought to halt fibrosis in the BLM model, they employed male and female mice younger than 12 weeks as recipients and young stem cell donors. [6, 7, 9, 25, 40–42] Previously it has been proposed that BM-MSCs therapy inhibits the progression of BLM-induced pulmonary fibrosis by altering both the inflammatory response and collagen deposition [6, 7, 9, 40] – an effect found to be age-dependent in pooled BM-MSCs isolated from young and aged mice and utilized in an LPS lung injury model of ARDS. [19] It should be noted however, that this study by Bustos et al. did not directly address the fibrotic process. In our analysis, a BLM-induced increase in TGF β , a key profibrotic growth factor found to be directly associated with IPF in prior literature [43], was prevented by infusion of γ ASCs. γ ASC infusion after BLM treatment also inhibited lung TNF α mRNA expression, an inflammatory marker, when compared to mice receiving BLM alone.

Pulmonary fibrosis may develop due to the activation of a profibrotic feedback loop that enhances collagen deposition/ECM turnover. [38] Increased activity of MMPs is directly associated with ECM turnover in IPF [13, 44, 45] and in other fibrotic diseases. [46–48] Higher MMP-2/9 activity and expression has been demonstrated in young [49] and aged mice [13] following BLM infusion. Although we focused on MMP-2, it should be pointed out that current studies suggest that multiple MMPs (1, 2, 7, 9, and 13) are important to the pathogenesis of IPF. [44] Our study confirms that lung tissue MMP-2 activity is higher after BLM instillation compared to saline controls. Furthermore, lung tissue MMP-2 activity in mice treated with BLM followed by γ ASCs was comparable to activity seen in mice receiving saline alone. On the other hand, MMP-2 activity remained elevated in mice receiving α ASCs.

The levels of MMP-2 activity directly correlate with the severity of fibrosis in young mice. [49] Similarly, increased expression of α_v -integrin, a potential activator of MMPs, [50] correlates with increased lung fibrosis in young mice, [36] as seen in the current aged male BLM model. Importantly, we found that expression of α_v -integrin mRNA is lower in donor γ ASCs compared to donor α ASCs at baseline. In addition, expression of TNF α mRNA, which is increased after BLM instillation in our model, has been shown to regulate MMP activity in other organ systems. [51] These data are supported by the current findings that

MMP-2 mRNA expression and activity was increased in ASCs isolated from old mice and old humans when compared to ASCs from young donor.

Among the multiple signaling pathways that could underlie the differences in the pro-fibrotic responses to BLM, we found increased baseline IGFR mRNA expression in donor oASCs compared to donor yASCs, which may be important since IGFR mediates AKT activation and AKT regulates vascular smooth muscle cell MMP-2 expression. [52] Similarly, we found that BLM-induced AKT phosphorylation in the aged mouse lung, was inhibited by donor yASC infusion. These data suggest that inhibition of the AKT pathway could be a mechanism by which donor yASCs inhibit the development of fibrosis and changes in MMP-2. Although AKT phosphorylation has been associated with severity of pulmonary fibrosis, [53· 54] a recent study of profibrotic lung fibroblasts (Thy-1) showed improved cell survival with increased pAKT levels. [37] Studies to examine this pathway in detail are ongoing in our laboratory.

Oxidant stress has been implicated in fibrotic lung diseases including IPF. [55] At baseline, measurements of ROS levels were lower in mice receiving BLM+yASCs compared to mice receiving BLM alone or BLM+oASCs. No difference was seen in measurements of ROS levels from lungs of mice receiving saline and those receiving BLM; we attribute this however, to the high baseline ROS associated with aging. Oxidative stress has been linked to MMP regulation, as gene expression and activation of proenzymes. MMP-1, 2, 7, and 9 are all activated by ROS via thiol group interactions. [56· 57] In addition, TGF β signaling can be initiated by ROS, ultimately increasing extracellular matrix protein (ECM) accumulation through direct up regulation of collagen synthesis and/or decreased matrix metalloproteinase activity. A recent report that blockade of both TGF- β 1/Smad2/3 and ROS signaling exerts an anti-fibrotic activity suggests a similar mechanism may be at play in our model following infusion of yASCs. [43]

Conversely, infusion of yASCs inhibited BLM-induced reduction of Nrf2 mRNA expression. Nrf2 regulates antioxidant gene expression, potentially contributing to the oxidant-antioxidant homeostasis in the injured pulmonary epithelium. [16] Thus, this finding may elucidate another mechanism of the anti-fibrotic action of yASCs. Our data are in agreement with Hecker et al., who demonstrated that fibrosis in aged, female mice receiving BLM could be reversed by targeting the Nox4-Nrf2 redox balance. [16] Further studies of yASCs will be necessary to dissect the targets of the Nrf2 pathway and to improve our understanding of the effects of aged on the imbalance between oxidants and antioxidants. [58· 59]

Finally, markers of apoptosis induced in the lungs of mice receiving BLM were inhibited by treatment with yASCs but not with oASCs. Oxidative stress is closely related to apoptosis in the progression of age-related fibrosis; however, recent literature suggests that “apoptosis resistance” contributes to worsened restrictive respiratory failure. [16] This phenomenon is also explained as an imbalance caused by the aging process since impaired apoptosis results in epithelial over-proliferation, followed by fibrosis. In previous studies, lungs of young mice receiving BLM showed increased levels of apoptosis markers when compared with lungs from saline control mice, presumably due to greater concentrations of damaged

epithelial cells. [11] However, lungs from aged mice were found to have fewer TUNEL-positive cells compared with the lungs of young mice. [16] In our study, higher levels of TUNEL-positive cells were seen in the lungs of mice receiving BLM compared to lungs of saline control mice. This finding was ameliorated by treatment with γ ASCs. Similarly, expression of cleaved Caspase-9 was seen to be highest in the lungs of mice receiving BLM alone.

Previous investigations found that young mice receiving BLM begin to undergo spontaneous resolution of pulmonary fibrosis beginning on day 21 post-instillation on histologic evaluation and quantification of collagen content. [18-39] Resolution appears to be complete by day 56. [60] Following infusion of oASCs in young mice, however, we observed higher levels of collagen content and integrin compared to untreated, young BLM mice. Therefore, we conclude that the administration of oASCs altered the course of resolution, which would have been expected in young BLM treated mice. [18-39-60] We demonstrated the injection of oASCs leads to the lack of therapeutic benefits when used in aged BLM mice, whereas the injection of γ ASCs prevents BLM-induced pulmonary fibrosis.

This study is the first to investigate the donor age-dependent effects of ASCs in modulating BLM-induced fibrosis in an aged mouse model. One study reported the use of BM-MSCs in acute lung injury using aged mice, [19] and another used ASCs in young BLM-treated mice. [40] Although expression of tissue factor-4 (TF-4) has been reported to be higher after ASC treatment, [61] raising concerns regarding the development of pulmonary emboli, we found no differences in lung TF-4 mRNA expression between any of the mice. Ongoing studies are currently comparing BM-MSCs and ASCs in aged mice.

Parker et al. suggest that age related decline of lung function may be related to dysfunctional ECM in a profibrotic environment, impairment of alveolar epithelial turnover in the apoptotic pathway, and oxidant/antioxidant imbalance. [38] Our data suggest that these mechanisms in the injured lung may be favorably altered by γ ASCs. In the absence of the BLM fibrotic stimuli (saline control mice), oASCs increased Ashcroft scoring without altering other fibrotic markers in the current study. Thus, subclinical fibrosis (found in the aged mouse lung) may affect the lung response to injury. Characterization of these changes may inform future investigations.

Our results demonstrate that γ ASCs have the ability, in contrast to oASCs, to regulate multiple growth factors and signaling pathways to inhibit fibrosis in the aged animal. Clearly, there are age-dependent, anti-fibrotic properties of γ ASCs. Clinical trials currently in progress in patients with IPF are focused on these areas. Whether the oASCs have acquired pro-fibrotic factors or lost anti-fibrotic factors remain to be studied. Additional preclinical studies are in progress as we explore MSCs as a potential therapy for human fibrotic lung diseases.

Acknowledgments

All authors have no disclosures regarding financial or personal relationships that could potentially influence the described research. All authors have read the journal's policy on disclosure of potential conflicts of interest. All

authors have read the journal's authorship agreement. This manuscript has been reviewed by and approved by all named authors. The authors thank the Lester and Sue Smith Foundation for their generous support in research funding. Authors SJE and PC were supported, in part, by the National Institute of Aging (R01 AG017170).

Abbreviations

IPF	idiopathic pulmonary fibrosis
BLM	bleomycin
MMP	matrix metalloproteinase
MSC	mesenchymal stem cell
ASC	adipose-derived mesenchymal stem cell
BM-MSC	bone marrow-derived mesenchymal stem cell
oASC	old-donor ASC
yASC	young-donor ASC
TGFβ	Transforming growth factor β
TNFα	tumor necrosis factor alpha
VEGF	vascular endothelial growth factor
IGF	insulin-like growth factor
TUNEL	terminal deoxynucleotidyl transferase-mediated dUTP nick-end labeling
ROS	reactive oxygen species
FACS	fluorescence activated cell sorting

References

1. Raghu G, Collard HR, Egan JJ, et al. An official ATS/ERS/JRS/ALAT statement: idiopathic pulmonary fibrosis: evidence-based guidelines for diagnosis and management. *American journal of respiratory and critical care medicine*. 2011; 183:788–824. [PubMed: 21471066]
2. Fernandez IE, Eickelberg O. New cellular and molecular mechanisms of lung injury and fibrosis in idiopathic pulmonary fibrosis. *Lancet*. 2012; 380:680–8. [PubMed: 22901889]
3. Raghu G, Weycker D, Edelsberg J, Bradford WZ, Oster G. Incidence and prevalence of idiopathic pulmonary fibrosis. *American journal of respiratory and critical care medicine*. 2006; 174:810–6. [PubMed: 16809633]
4. Hunninghake GM. A new hope for idiopathic pulmonary fibrosis. *The New England journal of medicine*. 2014; 370:2142–3. [PubMed: 24836311]
5. Izbicki G, Segel MJ, Christensen TG, Conner MW, Breuer R. Time course of bleomycin-induced lung fibrosis. *International journal of experimental pathology*. 2002; 83:111–9. [PubMed: 12383190]
6. Ortiz LA, Gambelli F, McBride C, et al. Mesenchymal stem cell engraftment in lung is enhanced in response to bleomycin exposure and ameliorates its fibrotic effects. *Proceedings of the National Academy of Sciences of the United States of America*. 2003; 100:8407–11. [PubMed: 12815096]

7. Rojas M, Xu J, Woods CR, et al. Bone marrow-derived mesenchymal stem cells in repair of the injured lung. *American journal of respiratory cell and molecular biology*. 2005; 33:145–52. [PubMed: 15891110]
8. Chaudhary NI, Schnapp A, Park JE. Pharmacologic differentiation of inflammation and fibrosis in the rat bleomycin model. *American journal of respiratory and critical care medicine*. 2006; 173:769–76. [PubMed: 16415276]
9. Ortiz LA, Dutreil M, Fattman C, et al. Interleukin 1 receptor antagonist mediates the antiinflammatory and antifibrotic effect of mesenchymal stem cells during lung injury. *Proceedings of the National Academy of Sciences of the United States of America*. 2007; 104:11002–7. [PubMed: 17569781]
10. Aguilar S, Scotton CJ, McNulty K, et al. Bone marrow stem cells expressing keratinocyte growth factor via an inducible lentivirus protects against bleomycin-induced pulmonary fibrosis. *PloS one*. 2009; 4:e8013. [PubMed: 19956603]
11. Degryse AL, Tanjore H, Xu XC, et al. Repetitive intratracheal bleomycin models several features of idiopathic pulmonary fibrosis. *American journal of physiology Lung cellular and molecular physiology*. 2010; 299:L442–52. [PubMed: 20562227]
12. Redente EF, Jacobsen KM, Solomon JJ, et al. Age and sex dimorphisms contribute to the severity of bleomycin-induced lung injury and fibrosis. *American journal of physiology Lung cellular and molecular physiology*. 2011; 301:L510–8. [PubMed: 21743030]
13. Sueblinvong V, Neujahr DC, Mills ST, et al. Predisposition for disrepair in the aged lung. *The American journal of the medical sciences*. 2012; 344:41–51. [PubMed: 22173045]
14. Foskett AM, Bazhanov N, Ti X, et al. Phase-directed therapy: TSG-6 targeted to early inflammation improves bleomycin-injured lungs. *American journal of physiology Lung cellular and molecular physiology*. 2014; 306:L120–31. [PubMed: 24242012]
15. Leach HG, Chrobak I, Han R, Trojanowska M. Endothelial cells recruit macrophages and contribute to a fibrotic milieu in bleomycin lung injury. *American journal of respiratory cell and molecular biology*. 2013; 49:1093–101. [PubMed: 23885794]
16. Hecker L, Logsdon NJ, Kurundkar D, et al. Reversal of persistent fibrosis in aging by targeting Nox4-Nrf2 redox imbalance. *Science translational medicine*. 2014; 6:231ra47.
17. Peng R, Sridhar S, Tyagi G, et al. Bleomycin induces molecular changes directly relevant to idiopathic pulmonary fibrosis: a model for “active” disease. *PloS one*. 2013; 8:e59348. [PubMed: 23565148]
18. Redente EF, Keith RC, Janssen W, et al. Tumor necrosis factor-alpha accelerates the resolution of established pulmonary fibrosis in mice by targeting profibrotic lung macrophages. *American journal of respiratory cell and molecular biology*. 2014; 50:825–37. [PubMed: 24325577]
19. Bustos ML, Huleihel L, Kapetanaki MG, et al. Aging mesenchymal stem cells fail to protect because of impaired migration and antiinflammatory response. *American journal of respiratory and critical care medicine*. 2014; 189:787–98. [PubMed: 24559482]
20. Barkauskas CE, Cronce MJ, Rackley CR, et al. Type 2 alveolar cells are stem cells in adult lung. *The Journal of clinical investigation*. 2013; 123:3025–36. [PubMed: 23921127]
21. Selman M, Pardo A. Role of epithelial cells in idiopathic pulmonary fibrosis: from innocent targets to serial killers. *Proceedings of the American Thoracic Society*. 2006; 3:364–72. [PubMed: 16738202]
22. Richeldi L, du Bois RM, Raghu G, et al. Efficacy and safety of nintedanib in idiopathic pulmonary fibrosis. *The New England journal of medicine*. 2014; 370:2071–82. [PubMed: 24836310]
23. Kotton DN, Morrisey EE. Lung regeneration: mechanisms, applications and emerging stem cell populations. *Nature medicine*. 2014; 20:822–32.
24. Huang K, Kang X, Wang X, et al. Conversion of bone marrow mesenchymal stem cells into type II alveolar epithelial cells reduces pulmonary fibrosis by decreasing oxidative stress in rats. *Molecular medicine reports*. 2014
25. Garcia O, Carraro G, Turcatel G, et al. Amniotic fluid stem cells inhibit the progression of bleomycin-induced pulmonary fibrosis via CCL2 modulation in bronchoalveolar lavage. *PloS one*. 2013; 8:e71679. [PubMed: 23967234]

26. Villeda SA, Plambeck KE, Middeldorp J, et al. Young blood reverses age-related impairments in cognitive function and synaptic plasticity in mice. *Nature medicine*. 2014; 20:659–63.
27. Paul SM, Reddy K. Young blood rejuvenates old brains. *Nature medicine*. 2014; 20:582–3.
28. Feng Z, Plati AR, Cheng QL, et al. Glomerular aging in females is a multi-stage reversible process mediated by phenotypic changes in progenitors. *The American journal of pathology*. 2005; 167:355–63. [PubMed: 16049323]
29. Furuichi K, Shintani H, Sakai Y, et al. Effects of adipose-derived mesenchymal cells on ischemia-reperfusion injury in kidney. *Clinical and experimental nephrology*. 2012; 16:679–89. [PubMed: 22398959]
30. Saito S, Nakayama T, Hashimoto N, et al. Mesenchymal stem cells stably transduced with a dominant-negative inhibitor of CCL2 greatly attenuate bleomycin-induced lung damage. *The American journal of pathology*. 2011; 179:1088–94. [PubMed: 21741938]
31. Wang Q, Zhu H, Zhou WG, et al. N-acetylcysteine-pretreated human embryonic mesenchymal stem cell administration protects against bleomycin-induced lung injury. *The American journal of the medical sciences*. 2013; 346:113–22. [PubMed: 23085672]
32. Ashcroft T, Simpson JM, Timbrell V. Simple method of estimating severity of pulmonary fibrosis on a numerical scale. *Journal of clinical pathology*. 1988; 41:467–70. [PubMed: 3366935]
33. Karl M, Berho M, Pignac-Kobinger J, Striker GE, Elliot SJ. Differential effects of continuous and intermittent 17beta-estradiol replacement and tamoxifen therapy on the prevention of glomerulosclerosis: modulation of the mesangial cell phenotype in vivo. *The American journal of pathology*. 2006; 169:351–61. [PubMed: 16877338]
34. Potier M, Karl M, Zheng F, et al. Estrogen-related abnormalities in glomerulosclerosis-prone mice: reduced mesangial cell estrogen receptor expression and pro-sclerotic response to estrogens. *The American journal of pathology*. 2002; 160:1877–85. [PubMed: 12000739]
35. Glassberg MK, Choi R, Manzoli V, et al. 17beta-estradiol replacement reverses age-related lung disease in estrogen-deficient C57BL/6J mice. *Endocrinology*. 2014; 155:441–8. [PubMed: 24274985]
36. Henderson NC, Arnold TD, Katamura Y, et al. Targeting of alphav integrin identifies a core molecular pathway that regulates fibrosis in several organs. *Nature medicine*. 2013; 19:1617–24.
37. Sueblinvong V, Neveu WA, Neujahr DC, et al. Aging promotes pro-fibrotic matrix production and increases fibrocyte recruitment during acute lung injury. *Advances in bioscience and biotechnology*. 2014; 5:19–30. [PubMed: 24596659]
38. Parker MW, Rossi D, Peterson M, et al. Fibrotic extracellular matrix activates a profibrotic positive feedback loop. *The Journal of clinical investigation*. 2014; 124:1622–35. [PubMed: 24590289]
39. Chung MP, Monick MM, Hamzeh NY, et al. Role of repeated lung injury and genetic background in bleomycin-induced fibrosis. *American journal of respiratory cell and molecular biology*. 2003; 29:375–80. [PubMed: 12676806]
40. Lee SH, Lee EJ, Lee SY, et al. The effect of adipose stem cell therapy on pulmonary fibrosis induced by repetitive intratracheal bleomycin in mice. *Experimental lung research*. 2014; 40:117–25. [PubMed: 24624895]
41. Cargnoni A, Gibelli L, Tosini A, et al. Transplantation of allogeneic and xenogeneic placenta-derived cells reduces bleomycin-induced lung fibrosis. *Cell transplantation*. 2009; 18:405–22. [PubMed: 19622228]
42. Moodley Y, Atienza D, Manuelpillai U, et al. Human umbilical cord mesenchymal stem cells reduce fibrosis of bleomycin-induced lung injury. *The American journal of pathology*. 2009; 175:303–13. [PubMed: 19497992]
43. Park SA, Kim MJ, Park SY, et al. EW-7197 inhibits hepatic, renal, and pulmonary fibrosis by blocking TGF-beta/Smad and ROS signaling. *Cellular and molecular life sciences : CMLS*. 2015; 72:2023–39. [PubMed: 25487606]
44. Nkyimbeng T, Ruppert C, Shiomi T, et al. Pivotal role of matrix metalloproteinase 13 in extracellular matrix turnover in idiopathic pulmonary fibrosis. *PloS one*. 2013; 8:e73279. [PubMed: 24023851]
45. Kapetanaki MG, Mora AL, Rojas M. Influence of age on wound healing and fibrosis. *The Journal of pathology*. 2013; 229:310–22. [PubMed: 23124998]

46. Elliot SJ, Catanuto P, Espinosa-Heidmann DG, et al. Estrogen receptor beta protects against in vivo injury in RPE cells. *Experimental eye research*. 2010; 90:10–6. [PubMed: 19799898]
47. Glassberg MK, Elliot SJ, Fritz J, et al. Activation of the estrogen receptor contributes to the progression of pulmonary lymphangioliomyomatosis via matrix metalloproteinase-induced cell invasiveness. *The Journal of clinical endocrinology and metabolism*. 2008; 93:1625–33. [PubMed: 18285421]
48. Kassira N, Glassberg MK, Jones C, et al. Estrogen deficiency and tobacco smoke exposure promote matrix metalloproteinase-13 activation in skin of aging B6 mice. *Annals of plastic surgery*. 2009; 63:318–22. [PubMed: 19602952]
49. Cai Y, Zhu L, Zhang F, et al. Noninvasive monitoring of pulmonary fibrosis by targeting matrix metalloproteinases (MMPs). *Molecular pharmaceuticals*. 2013; 10:2237–47. [PubMed: 23607644]
50. Knoblauch A, Will C, Goncharenko G, Ludwig S, Wixler V. The binding of Mss4 to alpha-integrin subunits regulates matrix metalloproteinase activation and fibronectin remodeling. *FASEB journal : official publication of the Federation of American Societies for Experimental Biology*. 2007; 21:497–510. [PubMed: 17172637]
51. Rajashekhar G, Shivanna M, Kompella UB, Wang Y, Srinivas SP. Role of MMP-9 in the breakdown of barrier integrity of the corneal endothelium in response to TNF-alpha. *Experimental eye research*. 2014; 122:77–85. [PubMed: 24667088]
52. Choo S, Papandria D, Zhang Y, et al. Outcomes analysis after percutaneous abdominal drainage and exploratory laparotomy for necrotizing enterocolitis in 4,657 infants. *Pediatr Surg Int*. 2011; 27:747–53. [PubMed: 21400031]
53. Russo RC, Garcia CC, Barcelos LS, et al. Phosphoinositide 3-kinase gamma plays a critical role in bleomycin-induced pulmonary inflammation and fibrosis in mice. *Journal of leukocyte biology*. 2011; 89:269–82. [PubMed: 21048214]
54. Park S, Ahn JY, Lim MJ, et al. Sustained expression of NADPH oxidase 4 by p38 MAPK-Akt signaling potentiates radiation-induced differentiation of lung fibroblasts. *Journal of molecular medicine*. 2010; 88:807–16. [PubMed: 20396861]
55. Cheresh P, Kim SJ, Tulasiram S, Kamp DW. Oxidative stress and pulmonary fibrosis. *Biochimica et biophysica acta*. 2013; 1832:1028–40. [PubMed: 23219955]
56. Nelson KK, Melendez JA. Mitochondrial redox control of matrix metalloproteinases. *Free radical biology & medicine*. 2004; 37:768–84. [PubMed: 15304253]
57. Smith NJ, Chan HW, Osborne JE, Thomas WG, Hannan RD. Hijacking epidermal growth factor receptors by angiotensin II: new possibilities for understanding and treating cardiac hypertrophy. *Cellular and molecular life sciences : CMLS*. 2004; 61:2695–703. [PubMed: 15549170]
58. Ray PD, Huang BW, Tsuji Y. Reactive oxygen species (ROS) homeostasis and redox regulation in cellular signaling. *Cellular signalling*. 2012; 24:981–90. [PubMed: 22286106]
59. Stadtman ER. Role of oxidant species in aging. *Current medicinal chemistry*. 2004; 11:1105–12. [PubMed: 15134509]
60. Schiller HB, Fernandez IE, Burgstaller G, et al. Time- and compartment-resolved proteome profiling of the extracellular niche in lung injury and repair. *Molecular systems biology*. 2015; 11:819. [PubMed: 26174933]
61. Tatsumi K, Ohashi K, Matsubara Y, et al. Tissue factor triggers procoagulation in transplanted mesenchymal stem cells leading to thromboembolism. *Biochemical and biophysical research communications*. 2013; 431:203–9. [PubMed: 23313481]

Background

Bleomycin-induced pulmonary fibrosis has been demonstrated to resolve spontaneously in young mice, but not old mice. An evaluation of age-dependent factors influencing the therapeutic benefits of mesenchymal stem cell has yet to be performed in a model for chronic lung fibrosis.

Translational significance

In the current study, young-donor adipose-derived stem cells (ASCs) demonstrated a therapeutic benefit in preventing bleomycin-induced pulmonary fibrosis in aged male mice, while old-donor ASCs were ineffective. This finding has important implications in the treatment of idiopathic pulmonary fibrosis, a disease primarily affecting men over 60 years of age, as clinical trials infusing mesenchymal stem cells are currently underway.

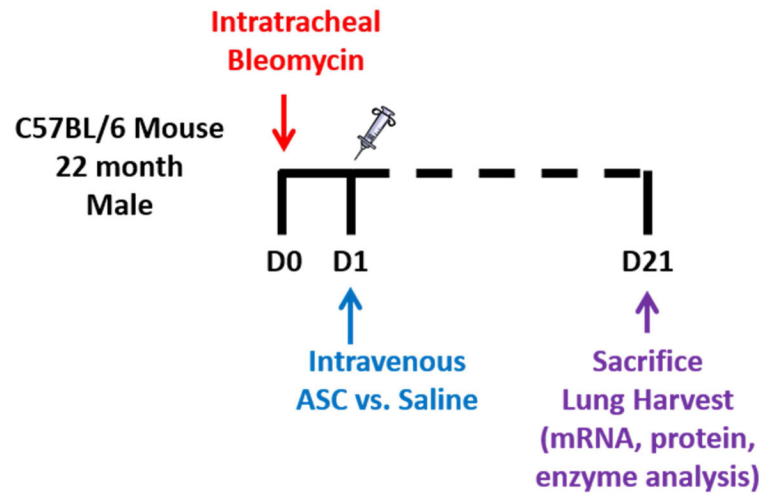


Figure 1. Schematic diagram of treatment Day 0 (D0)=time of bleomycin instillation. Day 1 (D1)=infusion of either saline or ASCs. Day 21(D21)=sacrifice.

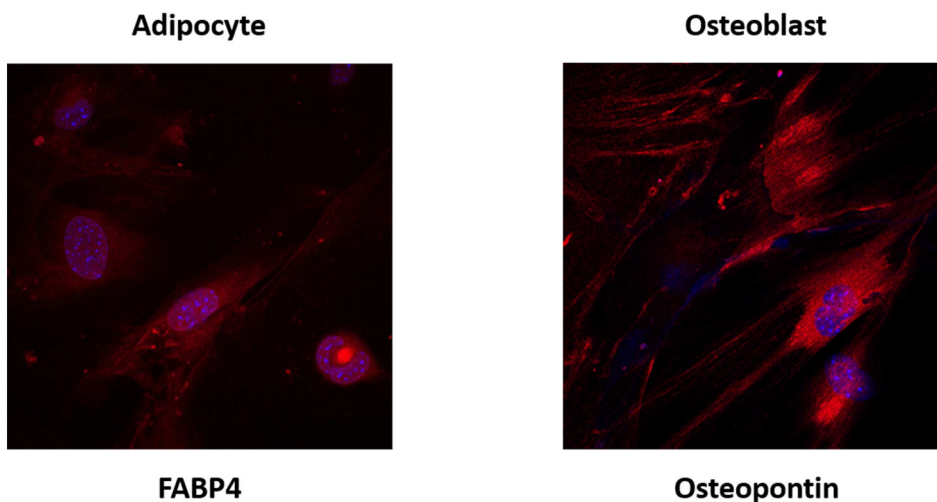


Figure 2. Adipose-derived mesenchymal stem cells (ASCs) isolated from 4 month and 22 month old male C57BL/6 mice demonstrate adipogenic and osteogenic differentiation potential
The mouse mesenchymal stem cell functional identification kit (R&D Systems, Minneapolis, MN) was used to stimulate differentiation of ASCs into adipocytes (left) and osteoblasts (right), per the manufacturer's instructions. Briefly, adipocytes were stained using goat anti-mouse FABP4 primary antibody, and osteocytes were stained using goat anti-mouse osteopontin primary antibody. Subsequently, both were exposed to donkey anti-goat IgG affinity purified PAb NorthernLights 557 fluorochrome-labeled secondary antibody (R&D Systems). Immunocytochemical staining of differentiated cells are presented with DAPI (blue) and NorthernLights (red) fluorescence imaging at magnification 40x.

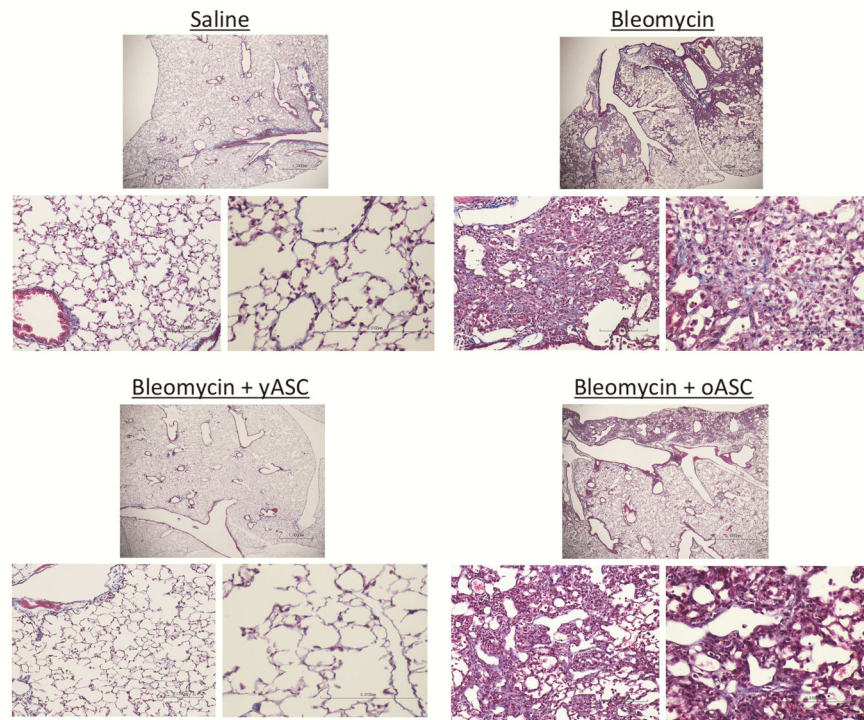


Figure 3. Bleomycin (BLM) pulmonary fibrosis in 22 month old male C57BL/6 mice is inhibited by young (yASC) but not old ASCs (oASC) at 21 day sacrifice
 Histologic examination of Masson's-Trichrome stained lung tissue was performed as described in Methods. Representative photomicrographs of the lungs of 22 month male C57BL/6 mice infused with saline (n=8), BLM (n=8), BLM+yASCs (n=7), or BLM+oASCs (n=9). Trichrome stained images at 2× (upper), 20× (left), and 40× (right) magnification.

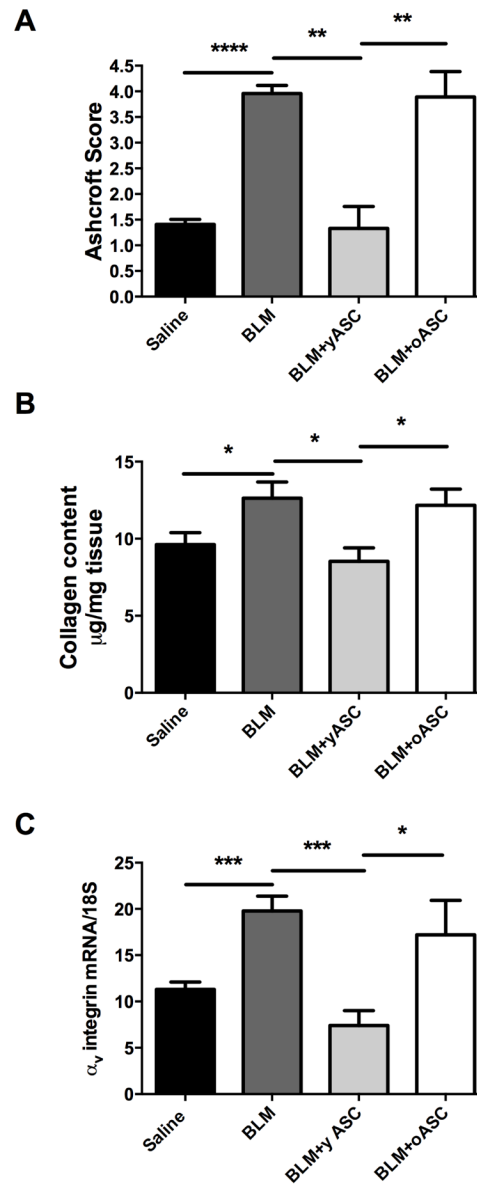
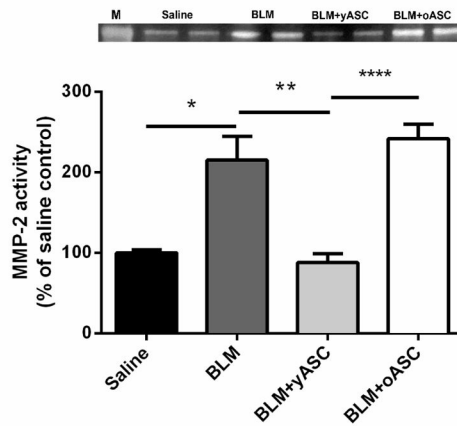


Figure 4. Bleomycin (BLM)-induced increase in markers of pulmonary fibrosis in the lungs of old male C57BL/6 are only inhibited by young adipose derived mesenchymal stem cells (yASC) not old ASCs (oASC)

A) Ashcroft scores were used to evaluate the degree of fibrosis. Data are graphed as the mean score of 32 fields/section of lung. Saline (n=8), BLM (n=8), BLM+yASCs (n=5), BLM+oASCs (n=7). **B)** Collagen content was estimated by hydroxyproline assay as described in methods. Data are graphed as µg/mg of lung tissue. Saline (n=8), BLM (n=8), BLM+yASCs (n=7), BLM+oASCs (n=8). **C)** α_v -integrin mRNA expression was determined by RT-PCR as a marker of fibrosis. Data are graphed normalized for 18S content. Saline (n=7), BLM (n=12), BLM+yASCs (n=5), BLM+oASCs (n=5), *p<0.05, **p<0.01, ***p<0.001, ****p<0.0001.

A



B

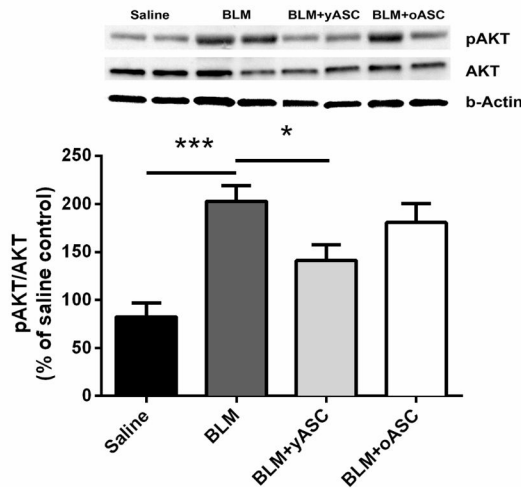
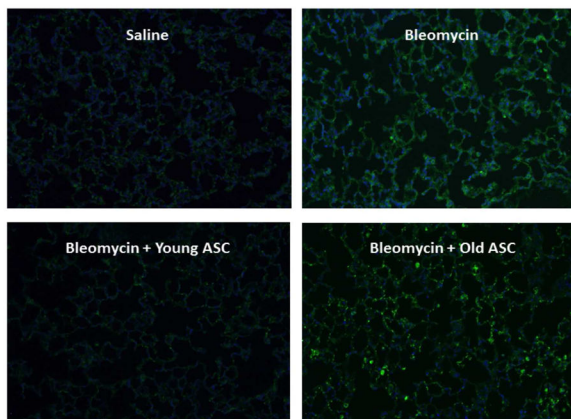


Figure 5. Bleomycin (BLM)-induced MMP-2 activity and AKT phosphorylation are inhibited in the lungs of aged male C57BL/6 mice by infusion of young adipose derived mesenchymal stem cells (yASC) but not old ASCs (oASC)

A) Zymography was performed on lung tissue protein extracts from aged male C57BL/6 mice receiving saline, BLM, BLM+yASC, or BLM+oASC to measure MMP-2 activity. A representative zymogram is shown of two individual mice/group. Data are graphed as the mean \pm SEM of n=5–6/group. **B)** Western blots were performed on lung tissue protein extracts from aged male C57BL/6 mice receiving saline, BLM, BLM+yASC, or BLM+oASC to measure AKT phosphorylation. A representative Western blot is shown of two individual mice/group. Data are graphed as the mean \pm SEM of n=5–9/group. * p<0.05, **p<0.01, ***p<0.001, ****p<0.0001.

A



B

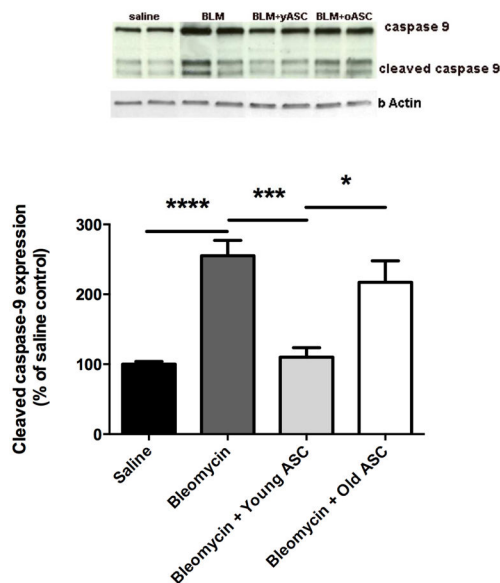


Figure 6. Markers of apoptosis are increased in lung tissue of aged male C57BL/6 after bleomycin (BLM) fibrosis, and inhibited by infusion of young adipose derived mesenchymal stem cells (yASC) but not old ASCs (oASC)

A) ApoptTag assay was performed on lung tissue sections from aged male C57BL/6 mice receiving saline, bleomycin (BLM), BLM+yASC, or BLM+oASC. Panels are stained with FITC (nuclear TUNEL labeling) and DAPI (nuclear staining) as indicated in the Methods section. **B)** Western blots were performed on lung tissue protein extracts from aged male C57BL/6 mice receiving saline, BLM, BLM+yASC, or BLM+oASC to measure the ratio of cleaved caspase-9 relative to total caspase-9. A representative Western blot is shown of two individual mice/group. Data are graphed as the mean \pm SEM of $n=4-10$ /group. * $p<0.05$, *** $p<0.001$, **** $p<0.0001$.

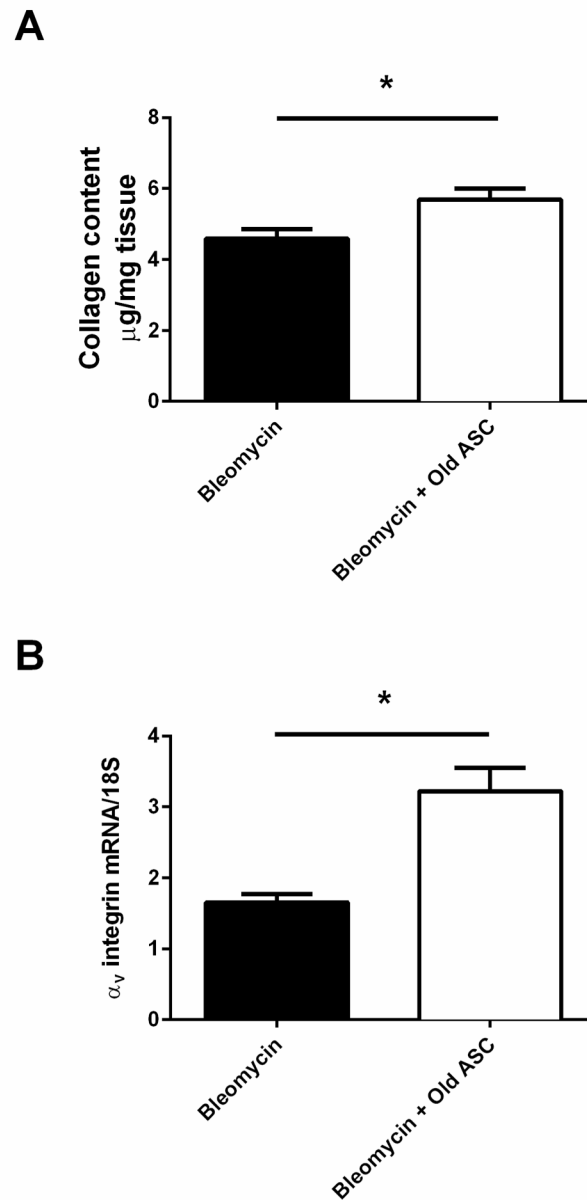


Figure 7. Old adipose derived mesenchymal stem cells (oASC) prevent or slow resolution of Bleomycin (BLM)-induced pulmonary fibrosis in the lungs of young male C57BL/6 mice
A) Collagen content was estimated by hydroxyproline assay as described in methods. Data are graphed as $\mu\text{g}/\text{mg}$ of lung tissue. **B)** α_v -integrin mRNA expression was determined by RT-PCR as a marker of fibrosis. Data are graphed normalized for 18S content. * $p < 0.05$. $n = 5$ individual mice for BLM, $n = 7$ individual mice for BLM+oASC.

Table 1
Flow-assisted cell sorting (FACS) analysis used to verify pluripotent potential of murine adipose-derived stem cells (ASCs) used for therapeutic injections

Cells isolated from subcutaneous fat were cultured on plastic Thermo Scientific™ Nunc™ Cell Culture Treated Flasks with Filter Caps (Thermo Fisher Scientific, Inc., Waltham, MA). Cells were counted and incubated with fluorescence-tagged, mouse-specific antibodies as listed above. Cellular markers were incubated without light and washed with phosphate buffer solution. Subsequently, the samples were analyzed on a FACS Canto™ II. CD 105 is a cell surface marker known to demonstrate heterogeneity between ASC samples. Based on percentage positivity, cellular markers were determined to be positive or negative for each cell line used for therapeutic injection.

Cellular marker	Polarity	oASC	yASC
CD 90.2	+	92.6%	85.8%
CD 105	+	0.2%	5.5%
CD 29	+	77.0%	66.7%
Sca-1	+	70.6%	69.5%
CD79 α	-	0.5%	0.9%
CD45	-	0.3%	0.6%
CD14	-	7.3%	7.0%
CD11	-	0.4%	1.5%

Table 2
Effect of Bleomycin (BLM) on inflammatory markers and oxidative stress in the lung

Vascular endothelial growth factor (VEGF) mRNA expression decreased in lungs from BLM mice compared to mice receiving saline; BLM mice treated with yASCs did not differ from BLM mice treated with oASCs. Infusion of yASC inhibited BLM-induced increase in tumor necrosis factor alpha (TNF α) mRNA expression; these mice had the same TNF α expression as saline controls. An age associated increase in lung ROS was inhibited only by infusion of yASC, not oASCs. BLM induced a reduction of lung nuclear factor erythroid 2-related factor 2 (Nrf2) mRNA expression compared to saline treatment, which was inhibited by infusion of yASCs. Transforming growth factor beta (TGF β) also demonstrated a BLM-induced increase, which was inhibited by yASC infusion.

Treatment Groups	VEGF mRNA/18S	TNF α mRNA/18S	ROS	Nrf2 mRNA/18S	TGF β mRNA/18S
Saline, n=3-6	4.54 \pm 0.78	0.18 \pm 0.09	18.5 \pm 0.68	19.0 \pm 3.65	6.57 \pm 1.80
BLM, n=5-11	0.51 \pm 0.04 ^a	3.43 \pm 1.02 ^a	18.6 \pm 0.52	8.47 \pm 1.11 ^a	19.5 \pm 2.49 ^a
BLM+yASC, n=3-8	1.01 \pm 0.33 ^a	0.80 \pm 0.34 ^b	13.3 \pm 1.25 ^{a,b}	18.3 \pm 1.83 ^b	2.63 \pm 1.47 ^b
BLM+oASC, n=5-11	0.61 \pm 0.11 ^a	0.38 \pm 0.07 ^{a,b}	18.4 \pm 1.20 ^c	8.82 \pm 1.24 ^{a,c}	18.0 \pm 3.17 ^c

^a p<0.05 compared to saline;

^b p<0.05 compared to BLM;

^c compared to yASC. Values are expressed as mean \pm standard error of mean.